AIP | Journal of Applied Physics

X-ray absorption fine structure and electron energy loss spectroscopy study of silicon nanowires at the Si L 3,2 edge

X.-H. Sun, Y.-H. Tang, P. Zhang, S. J. Naftel, R. Sammynaiken, T. K. Sham, H. Y. Peng, Y.-F. Zhang, N. B. Wong, and S. T. Lee

Citation: Journal of Applied Physics **90**, 6379 (2001); doi: 10.1063/1.1417997
View online: http://dx.doi.org/10.1063/1.1417997
View Table of Contents: http://scitation.aip.org/content/aip/journal/jap/90/12?ver=pdfcov
Published by the AIP Publishing

Articles you may be interested in

DNA-modified silicon nanocrystals studied by X-ray luminescence and X-ray absorption spectroscopies: Observation of a strong infra-red luminescence band
J. Appl. Phys. **111**, 054311 (2012); 10.1063/1.3691600

The spatial resolution of electron energy loss and x-ray absorption fine structure
J. Appl. Phys. **104**, 034906 (2008); 10.1063/1.2960582

Structure and electronic properties of SiO 2 / Si multilayer superlattices: Si K edge and L 3,2 edge x-ray absorption fine structure study
J. Appl. Phys. **92**, 3000 (2002); 10.1063/1.1501742

Phosphorus-doped silicon nanowires studied by near edge x-ray absorption fine structure spectroscopy
Appl. Phys. Lett. **80**, 3709 (2002); 10.1063/1.1478796

Luminescent intrazeolitic Si nanoclusters: Size study by Si K and L 2,3 x-ray absorption near-edge structure, x-ray photoelectron and photoluminescence spectroscopies
Appl. Phys. Lett. **71**, 3194 (1997); 10.1063/1.120287

Reuse of AIP Publishing content is subject to the terms at: https://publishing.aip.org/authors/rights-and-permissions. Download to IP: 129.173.74.49 On: Wed, 08 Jun 2016 15:03:44

X-ray absorption fine structure and electron energy loss spectroscopy study of silicon nanowires at the Si $L_{3,2}$ edge

X.-H. Sun,[a] Y.-H. Tang, P. Zhang, S. J. Naftel, R. Sammynaiken, and T. K. Sham[b]
Department of Chemistry, University of Western Ontario, London, Canada N6A 5B7

H. Y. Peng, Y.-F. Zhang, N. B. Wong, and S. T. Lee
Center Of Super-Diamond and Advanced Films (COSDAF) and Department of Physics and Materials Science, The City University of Hong Kong, Hong Kong SAR, China

(Received 2 July 2001; accepted for publication 14 September 2001)

X-ray absorption fine structures (XAFS) and electron energy loss spectroscopy (EELS) at the Si $L_{3,2}$ edge have been used to investigate a series of Si nanowires (as-prepared and HF refreshed). X-ray excited optical luminescence (XEOL) was also used to study the optical properties of these Si nanowires. Although no noticeable edge-jump blueshift (widened band gap) is observed in XAFS, a noticeable change in the edge jump (a less steep rise and the blurring of spectral features) is observed, indicating considerable degradation in the long-range order and size effects. However, EELS with a nanobeam exhibits a threshold blueshift and parabolic behavior for some selected wires indicating that there are grains smaller than the nominal diameter in these nanowires. Thus, XAFS probes the average of a distribution of wires of various sizes of which the majority is too large to exhibit detectable quantum confinement behavior (blueshift) observed and inferred in EELS and XEOL. The results and their implications are discussed. © *2001 American Institute of Physics.*
[DOI: 10.1063/1.1417997]

INTRODUCTION

Silicon in nanometer dimension has been a fascinating topic for research in many laboratories over the last decade. Of particular interest are the discovery of luminescence from porous silicon (PS), a sponge-like silicon comprising an interconnecting network of crystalline silicon nanowires with pillars and nodules of nm size[1] and more recently, the synthesis of bulk quantity of Si nanowires.[2–4] The PS luminescence is exciting in that bulk Si, an indirect band gap material, is not expected to luminesce in the visible. Also, getting silicon nanostructure to emit light has enormous technological implications.[5] There is now a large body of experimental and theoretical evidence[5] that shows that the origin of the luminescence from porous silicon is quantum confinement, modified, sometimes considerably, by surface and interface/grain-boundary chemistry,[5–7] although there is an ongoing debate on the details of the luminescence mechanism and the nature of the optical band gap.[5,8,9] Evidence for quantum confinement, i.e., widening of the band gap and observation of luminescence in the visible in PS[10,11] and related systems such as Si nanocrystallites[12–14] and Si/SiO_2 multilayer quantum wells[15,16] continues to mount.

The recent development of laser ablation and thermal evaporation techniques[2–4] enables the fabrication of bulk quantities of free-standing Si nanowires (NWs). These wires exhibit photoluminescence in the visible, albeit with considerably weaker luminosity compared to PS.[3,4] The luminescence property of Si nanowires is particularly interesting in that the diameter of these wires, as revealed from transmission electron microscopy (TEM) images, is several to tens of nm, and is generally too large to exhibit quantum confinement effects exhibited by Si nanostructures.[8–14] It is interesting to ask whether or not Si NW exhibits quantum confinement behavior. According to theory and experimental observations, a quantum confinement mechanism for luminescence from a nano Si crystallite normally requires a size of <5 nm.[5,8,12,13] Thus luminescence from nanowires must arise from grains or oxide-encapsulated nanocrystallites with a size of <5 nm in the wire or from defects in the oxide layer as well as defects induced by the surface and interface/grain boundary effects.[5] In this article, we report on a Si $L_{3,2}$ edge x-ray absorption fine structure (XAFS) and electron energy loss spectroscopy (EELS) study of bulk quantity, multi- and single nanowires to address these issues. $SiL_{3,2}$ edge XAFS measures the electronic structure of the unoccupied densities of states of primarily *s* character in the conduction band for a distribution of Si nanowires with a $\sim$ mm photon beam while EELS on the other hand can perform measurements with a nanobeam (tens of nm). This permits a site-specific study of a collection of several and even a single wire. X-ray excited optical luminescence (XEOL) using a Al $K\alpha$ x-ray source was used to confirm the photoluminescence of these specimens.

EXPERIMENT

Si nanowires investigated in this work were prepared using a laser ablation technique as described previously.[3,4] The procedure involves the use of an excimer laser (248 nm, 10 Hz, 400 mJ) to ablate a target of Si and SiO_2 mixture in

[a]Visiting from the City University of Hong Kong.
[b]Author to whom correspondence should be addressed; electronic mail: sham@uwo.ca

 © 2001 American Institute of Physics
Reuse of AIP Publishing content is subject to the terms at: https://publishing.aip.org/authors/rights-and-permissions. Download to IP: 129.173.74.49 On: Wed, 08 Jun 2016 15:03:44

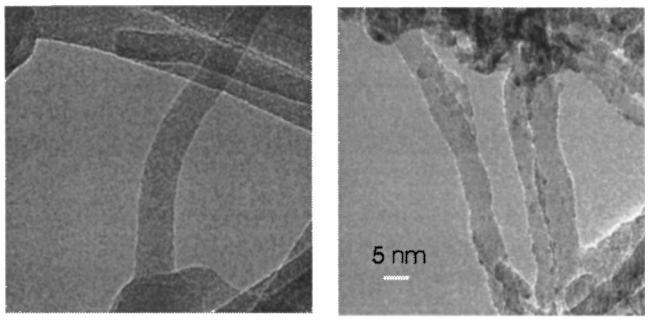

FIG. 1. (a) TEM of a single Si NW (~11 nm in diameter) from an ambient specimen. (b) TEM of Si NW (after HF etching) with diameters varying from 5 to 10 nm. Notice that the surface becomes rugged after etching and that nm nodules are clearly visible. The scale applies to both images.

an evacuated quartz tube. An inert carrier gas, normally Ar, is used and the cotton-like brownish nanowires are collected on the wall of the tube downstream near a cold finger.[3,4] The nanowires studied here had been characterized with SEM, energy dispersive x ray (EDX), TEM, x-ray powder diffraction, and x-ray absorption fine structure (XAFS) at the Si *K*-edge.[4,17] These wires are typically micron long with diameters varying from a few nm to tens of nm, depending on the preparation conditions and are usually encapsulated by a silicon oxide layer. For the purpose of discussion in this work, nominal diameter (size distribution maximum with a width at half maximum of ~5 nm) is used. Si nanowires of nominally ~13–~26 nm were used in the Si $L_{3,2}$ XAFS experiment. In EELS studies, multiple wires as well as a single wire with a specific size were selected with TEM prior to the EELS measurement. XEOL was obtained using both a laboratory Al $K\alpha$ x-ray source and synchrotron radiation. They both show that Si NW exhibit photoluminescence, albeit considerably weaker than porous silicon. The Al $K\alpha$ excitation results are reported below and the synchrotron results will be reported elsewhere.[18]

It has been established that Si NW prepared according to the above described procedure tends to grow along the (112) direction and crystal defects are common,[4] although some other direction has also been reported.[2] Si NW is often encapsulated with a relatively thick silicon oxide layer, which probably plays an important role in the one-dimensional growth.[4] For example, it is common to find that a ~25 nm diam Si nanowire has a ~5 nm oxide layer.[17] To remove the oxide layer and its effect, we etched the specimens with HF prior to the measurement. The surface of the HF-etched Si NW is H passivated. SEM, EDX, and TEM all show that this procedure removes the oxide layer without altering the morphology of the nanowires significantly. Figure 1 shows the TEM micrograph of representative Si nanowires of ~10 nm before [Fig. 1(a)] and after HF treatment [Fig. 1(b)]. It is worth noting that after HF etching, the morphology of the wires remains intact but the surface becomes very rough and modulates considerably. Small nodules are also visible.

Si $L_{3,2}$-edge XAS experiments were carried out at the grasshopper beamline of the Canadian Synchrotron Radiation Facility located at the Synchrotron Radiation Center, University of Wisconsin-Madison. A1800 l/mm grating was used. At a modest slit setting of 30 μm, the beamline provides a photon energy resolution of ~0.2 eV at the Si $L_{3,2}$ edge (~100 eV). The EELS experiments were carried out at the City University of Hong Kong using a Philips TEM system (Model FEG-TEM CM200) fitted with an EELS spectrometer. The TEM was operated at 200 kV using a beam current of ~0.5 nA and a spectral resolution of ~0.5 eV was used for the EELS. Si NW were placed onto a holey carbon grid and prepared according to standard procedure. Silicon nanowires, both stored in the ambient and etched with a HF solution prior to the measurement, were studied with XAFS at the Si $L_{3,2}$ edge and EELS at both the Si $L_{3,2}$ edge and O *K* edge. The energy of the EELS spectrum from different runs was calibrated with respect to the silicon oxide resonance, which is a very recognizable feature in Si $L_{3,2}$ edge XAFS.[19,20] In XAFS measurements, the beam size was ~1 mm×3 mm. In EELS, both 50 and 10 nm beam were used to measure a collection of multiple wires and a single nanowire, respectively. A TEM image of the area of interest (e.g., Fig. 1) was always taken prior to the EELS measurement. Thus the EELS data are site specific over a collection of several nanowires or a single nanowire, while XAFS measures the average over a large number and size distribution. In XAFS, both total electron yield (TEY) and fluorescence yields (FLY) were used. The sampling depth of TEY and FLY depends on the penetration depth of the incident photon and the energy dependent escape depth of yields (electrons and the fluorescent photons). At the Si $L_{3,2}$ edge, the one-absorption length above the edge is ~60 nm. This is long compared to the electron escape depth but shorter than the attenuation of the fluorescence photons.[19–21] Thus TEY is sensitive to the surface and near surface region of the wire, while FLY probes the surface as well as the "bulk".[19,20,21,22] At these low photon energies however, FLY suffers greatly from thickness effects (self-absorption and chemical inhomogeneity).[21]

The XEOL experiment was carried out in a customer built surface science chamber which was equipped with a set of lenses to collect and focus onto the entrance slit of a JY HA-100 monochromator. The luminescence was detected with a Hamamatsu photomultiplier tube (R943-02) as described previously.[20] The XEOL spectrum was obtained by removing the blackbody radiation background (from the x-ray filament) obtained with a nonluminescent substrate. This has little effect on specimens with strong luminescence such as porous silicon but has some effect (noisier in the 600–850 nm region) on the specimen of weak luminescence such as Si NW.

RESULTS AND DISCUSSION

Figure 2 shows the Si $L_{3,2}$ edge XAFS of two Si NW samples with nominal diameters of 26 and 13 nm together with that of a Si(100) wafer and a porous silicon. All specimens had been etched with HF prior to the measurement. The XAFS for the ambient Si nanostructures (not shown) are dominated by the oxide signal (see Fig. 4) and the presence of the oxide encapsulated, unoxidized portion of the Si NW

Reuse of AIP Publishing content is subject to the terms at: https://publishing.aip.org/authors/rights-and-permissions. Download to IP: 129.173.74.49 On: Wed, 08 Jun 2016 15:03:44

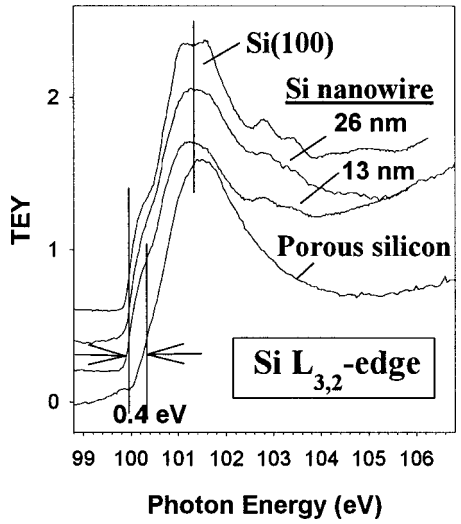

FIG. 2. Si $L_{3,2}$ edge XAS for two Si NW specimens together with those of Si(100) and porous silicon (p type, 20 mA, 20 min). The nominal diameters of 26 nm (main range: 22–30 nm) and 13 nm (main range: 11–15 nm) are noted. The vertical lines mark the threshold (inflection point).

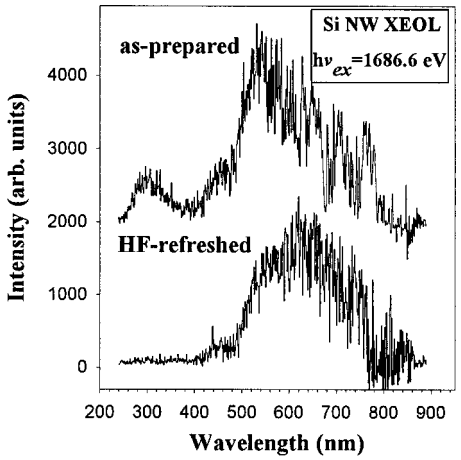

FIG. 3. X-ray excited optical luminescence (XEOL) of a Si nanowire specimen (nominal diameter 26 nm, before and after HF treatment) using an Al $K\alpha$ x-ray source. It exhibits luminescence in the ultraviolet and visible. The short wavelength peaks (~300 and ~450 nm) diminish after HF treatment while the 530 nm peak and longer wavelength emission remain.

is not always clearly noticeable. A couple of interesting features from Fig. 2 can be noted. First, there is no noticeable shift in the edge threshold (inflection point) of Si NW relative to Si(100) despite a less-steep edge-jump profile, while porous silicon exhibits a noticeable blueshift indicating the opening of the band gap as reported previously for Si nanostructures.[10–16] Second, the doublet features centred at ~101.5 and ~103 eV in the Si(100) spectrum become blurred in Si NW and disappear entirely in porous silicon. The doublet features in Si(100) arise from a dipole transition from the $2p$ shell ($2p_{3/2}$ and $3p_{1/2}$ separates by 0.6 eV) and band structure effects (there are in fact three sets of doublets, up to ~104 eV, corresponding to the unoccupied states of primarily s character in the conduction band Δ_1, L_1, and L_3 bands for example, the first two sets overlap slightly). A lack of or a blurred doublet is associated with the deterioration of long range order in the crystal lattice, surface effects, and chemical inhomogeneity.[17,20,22]

It is puzzling though not unexpected that the Si NW specimen exhibits no noticeable blueshift at the Si $L_{3,2}$ edge threshold (Fig. 2), as expected for quantum confinement. It is not unexpected because the nominal diameters of these nanowires are larger than the much smaller nodules in porous silicon and single nanocrystallites (<5 nm).[8,9,13,14] It is puzzling because all the quantum confined Si systems, such as porous silicon,[10,11] single Si nanocrystallites[12–14] and Si/SiO_2 quantum wells,[14,15] exhibit photoluminescence in the visible and band gap opening as measured in Si $L_{3,2}$ edge blueshifts among other techniques.[5] As noted above, these Si NW exhibit luminescence in the visible with synchrotron and Al $K\alpha$ x-ray excitation. A XEOL spectrum of the 26 nm specimen excited using an Al $K\alpha$ x-ray source clearly shows luminescence in both UV and visible (Fig. 3). Upon HF etching the luminescence at the shorter wavelengths (295 and 460 nm) diminishes but the visible (~530 nm and above) remains. This result indicates that as-prepared Si NW contains small unoxidized Si nanocrystallites that contribute to the luminescence, a quantum confinement behavior. The short wavelength luminescence probably has its origin from the presence of the oxide layer.[23] More experiments will be needed and the detailed analysis will be published elsewhere.[18] The lack of blueshift in the XAFS of the Si NW in Fig. 2 almost certainly arises from the fact that XAFS measures the average properties of a large number of Si NW of various sizes. It is conceivable that while only a certain portion of the Si NW specimen (grain size <5 nm) exhibits quantum confinement and contributes to the luminescence, the XAFS signal is dominated by the majority of larger nonluminescent crystallites in the wires. Thus, a nanobeam, site-selective EELS study would be needed to provide the much needed spatial resolution.

Figure 4 shows the Si $L_{3,2}$ edge and O K edge EELS from multiwires at various spots of an Si NW specimen (11–15 nm) from a HF refreshed (top spectrum) and an ambient sample (no HF refreshment) using a 50 nm beam (covering 3–5 wires). The spectral features characteristic of Si and SiO_2 absorption are marked with vertical lines. The first resonance (marked at the inflection point of the rising edge) at the Si $L_{3,2}$ edge corresponds to the $2p$ to s transition from the unoxidized Si to the bottom of the conduction band. Thus the position of the rising edge can be used to monitor the movement of the conduction band resulting from quantum confinement. Since all the unoxidized portion of the nanowires is essentially crystalline Si, no significant $2p$ core level chemical shift is expected and a blueshift of the position of the Si $L_{3,2}$ edge-jump relative to that of bulk Si can be associated with the upward movement of the conduction band upon decreasing size (evidence for quantum confinement). This movement is also reflected in the luminescence spectrum. The second resonance (marked at maximum intensity) is characteristic of Si in a tetrahedral oxygen environment (SiO_2). From the varying intensity of the Si and SiO_2 features, we can see that there is clearly a distribution of wires with varying size, surface oxide thickness, and orientation to a lesser extent (gauging from the relative intensity of Si and

Reuse of AIP Publishing content is subject to the terms at: https://publishing.aip.org/authors/rights-and-permissions. Download to IP: 129.173.74.49 On: Wed, 08 Jun 2016 15:03:44

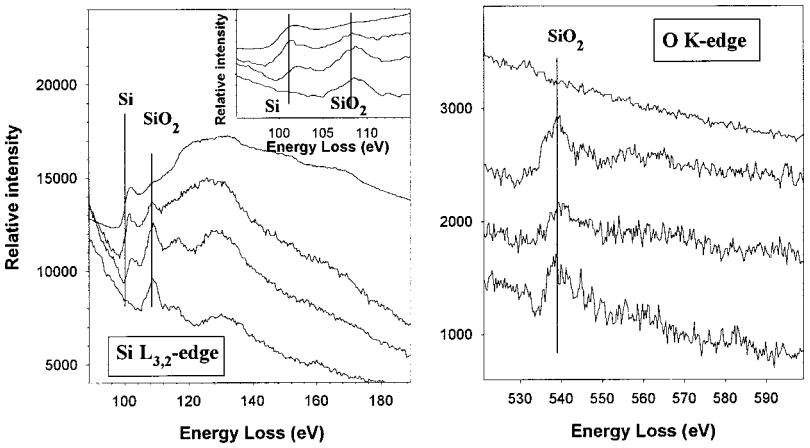

FIG. 4. EELS from a HF-refreshed (top spectrum) and several regions of an ambient Si NW specimen (~11–15 nm diameter) at the Si $L_{3,2}$ and the O K edge using a 50 nm beam. The characteristic edge resonances for Si and SiO_2 at the Si $L_{3,2}$ edge are marked with a vertical line. The inset shows a Si $L_{3,2}$ edge threshold blueshift in one of the areas examined.

SiO_2 peaks).[19] The O K edge spectra confirm the relative presence of oxide on these specimens. This observation is in good accord with high resolution TEM results.[4]

Perhaps the most interesting feature from Fig. 4 is that the presence of SiO_2 provides a convenient energy calibration. In the inset of Fig. 4 the SiO_2 resonance maximum is aligned. We can clearly see that the edge jump (inflection point) of one spectrum clearly exhibits a blueshift. This observation, together with the XEOL (Fig. 3) indicates that there exist nanocrystallites (quantum confined) in these nanowires, which are responsible for the optical luminescence. Figure 5 shows the Si $L_{3,2}$ edge EELS of three single wires with diameters of 50, 30, and 9 nm from a HF-etched Si NW specimen. All spectra were obtained in the same run under identical experimental conditions. The XAFS for an ambient Si(100) wafer recorded in TEY (surface sensitive) and FLY (bulk sensitive) are also shown. The edge jump (point of inflection) of the 50 nm wire is aligned with that of the XAFS of Si(100) and is used to represent the EELS of a larger Si NW where quantum confinement is least expected. In fact this spectrum is nearly identical to that of a Si standard. A more detailed comparison after the removal of a linear background is shown in the inset.

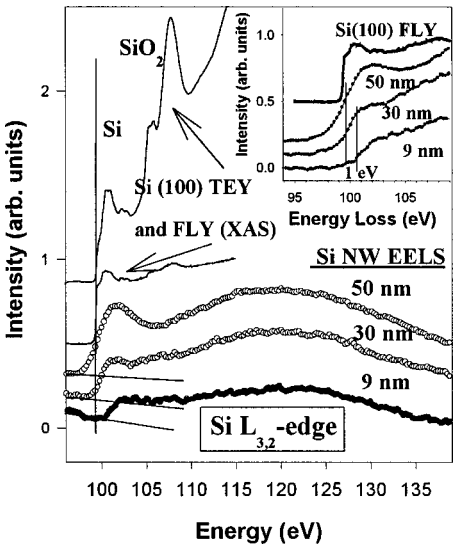

FIG. 5. EELS of three single Si nanowires of ~50, ~30, and 9 nm from a HF-etched Si NW specimen. The XAFS of a Si(100) wafer recorded in TEY and FLY mode are also shown. The edge jump of the 50 nm nanowires was aligned to that of the Si(100). All EELS spectra were recorded within the same run with identical experimental conditions. The pre-edge background is also shown. A more detailed comparison of the edge jump is shown in the inset.

Several features are worth noting. First, no oxide resonance in the 105–110 eV region is apparent. This indicates that the HF treatment effectively removed the surface oxide layer. Second, the edge profile for the nanowires is significantly broader compared to the XAFS edge jump of Si(100). This behavior is partly due to resolution and partly due to the size and polycrystalline effect. The behavior of the profile of the absorption edge as the size decreases resembles that of the single nanocrystallites reported by Batson and Heath[13] in that the edge jump becomes more parabolic and blurry as the size decreases. Third, there is clearly a blueshift at the threshold of the 9 nm spectrum accompanied by a more parabolic-like edge jump as judged by the disappearance of the valley at ~105 eV. Although the ~1 eV shift shown in Fig. 4 has large uncertainty (0.2 eV), the presence of a blueshift is clear. This observation immediately indicates the widening of the band gap in the area of the Si NW investigated. Similar behavior has been observed in related systems. Batson and Heath[13] showed that for a single Si nanocrystallite of less than 5.5 nm, the edge profile becomes more parabolic and blurry and shifts to higher energy as the size of the crystallite decreases further. Since the nominal diameter of the wire (9 nm) studied here is larger than the required size for a single nanocrystallite to exhibit the effect of quantum confinement, we propose that the presence of smaller grains in the 9 nm Si NW is responsible for the observed blueshift. Based on the effective mass model ($E(k) \propto (\hbar\pi)^2/2m^*R^2$) and the $1/R^2$ (R=radius of the grain) dependence of the shift of the bottom of the conduction band proposed by Batson and Heath,[13] we estimate that a ~1 eV shift corresponds to a grain size of ~2.5 nm and a lower bound of 590 nm for the optical gap. This estimate is in reasonable accord with theory[8] and experiment (Fig. 3).

SUMMARY AND CONCLUSION

We have reported an observation of the electronic and optical behavior of a series of Si nanowires using XAFS and

Reuse of AIP Publishing content is subject to the terms at: https://publishing.aip.org/authors/rights-and-permissions. Download to IP: 129.173.74.49 On: Wed, 08 Jun 2016 15:03:44

EELS measurements at the Si $L_{3,2}$ edge and XEOL with Al $K\alpha$ x-ray excitation. XAFS, a probe for average properties of a distribution of Si nanowires, shows that the oxide encapsulated Si in Si NW is crystalline and bulk-like, although there is evidence for a significant degradation of long range order. Spatially resolved EELS reveals a Si $L_{3,2}$ edge blueshift in some as-prepared Si NW and in a ~HF refreshed 9 nm Si NW. This observation is attributed to the presence of a small fraction of silicon nanocrystallite in Si NW, which exhibits quantum confinement behavior (band gap widening and luminescence in the visible). This behavior is not readily detected in a spatially average technique such as XAFS using a mm beam (unless a submicron beam from a third generation source is used). The properties are detectable however in spatially resolved and site-specific techniques such as EELS and XEOL, respectively.

ACKNOWLEDGMENTS

T.K.S. wishes to acknowledge the great hospitality of the City University of Hong Kong where he was a visitor. Research carried out at the University of Western Ontario was supported by the Natural Science and Engineering Research Council (NSERC) of Canada. S.R.C. is supported by the U.S. NSF under Grant No. DMR-00-84402. Research at COSDAF is supported by the Research Grants Council of Hong Kong (Project No. 9040459). The authors are in debted to K.H. Tan of CSRF for his technical assistance.

[1] L. T. Canham, Appl. Phys. Lett. **57**, 1046 (1990).
[2] A. M. Morales and C. M. Lieber, Science **279**, 208 (1998).
[3] Y. F. Zhang, Y. H. Tang, N. Wang, D. P. Yu, C. S. Lee, I. Bello, and S. T. Lee, Appl. Phys. Lett. **72**, 1835 (1998).
[4] S. T. Lee, N. Wang, Y. F. Zhang, and Y. H. Tang, MRS Bull. **24**, 36 (1999).
[5] A. G. Cullis, L. T. Canham, and P. D. J. Calcott, J. Appl. Phys. **82**, 909 (1997).
[6] M. V. Wolkin, J. Jorne, P. M. Fauchet, G. Allan, and C. Delerue, Phys. Rev. Lett. **82**, 197 (1999).
[7] I. Coulthard and T. K. Sham, Solid State Commun. **110**, 203 (1999).
[8] S. Öğüt, J. R. Chelikowsky, and S. G. Louie, Phys. Rev. Lett. **79**, 1770 (1997).
[9] G. Allan, C. Delerue, and M. Lannoo, Phys. Rev. Lett. **76**, 2961 (1996).
[10] T. van Buuren, Y. Gao, T. Tiedje, J. R. Dahn, and B. M. Way, Appl. Phys. Lett. **60**, 3013 (1992).
[11] T. K. Sham *et al.* Nature (London) **363,** 331 (1993).
[12] K. A. Littau, P. J. Szajowski, A. J. Muller, A. R. Kortan, and L. E. Brus, J. Phys. Chem. **97**, 1224 (1993).
[13] P. E. Batson and J. R. Heath, Phys. Rev. Lett. **71**, 911 (1993).
[14] J. P. Wilcoxon and G. A. Samara, Appl. Phys. Lett. **74**, 3164 (1999).
[15] Z. H. Lu, D. J. Lockwood, and J.-M. Barbeau, Nature (London) **378**, 258 (1995).
[16] D. J. Lockwood, Z. H. Lu, and J.-M. Barbeau, Phys. Rev. Lett. **76**, 539 (1996).
[17] Y. F. Zhang, L. S. Liao, W. H. Chan, R. Sammynaiken, T. K. Sham, and S. T. Lee, Phys. Rev. B **61**, 8298 (2000).
[18] S. J. Naftel *et al.* (unpublished results).
[19] M. Kasrai, W. N. Lennard, R. W. Brunner, G. M. Bancroft, J. A. Bardwell, and K. H. Tan, Appl. Surf. Sci. **99**, 303 (1996).
[20] T. K. Sham and I. Coulthard, J. Synchrotron Radiat. **6**, 215 (1999).
[21] T. K. Sham, S. J. Naftel, and I. Coulthard, in *Chemical Applications of Synchrotron Radiation*, edited by T. K. Sham (World Scientific, Singapore, in press).
[22] T. K. Sham, X-H. Feng, D.-T. Jiang, B. X. Yang, J. Z. Xiong, A. Bzowski, D. C. Houghton, B. Bryskiewicz, and E. Wang, Can. J. Phys. **70**, 813 (1992).
[23] S. J. Naftel, I. Coulthatd, D. T. Jiang, T. K. Sham, B. W. Yates, and K. H. Tan, Phys. Status Solidi **181**, 373 (2000).

Reuse of AIP Publishing content is subject to the terms at: https://publishing.aip.org/authors/rights-and-permissions. Download to IP: 129.173.74.49 On: Wed, 08 Jun 2016 15:03:44